Heliyon 9 (2023) e18755

Contents lists available at ScienceDirect

Heliyon

journal homepage: www.cell.com/heliyon

Houttuynia cordata Thunb. Hexane fraction induces MDA-MB-231 cell apoptosis via caspases, ER stress, cell cycle arrest and attenuated Akt/ERK signaling

Pitsinee Inthi [a], Hataichanok Pandith [b,c], Prachya Kongtawelert [a], Subhawat Subhawa [a], Ratana Banjerdpongchai [a,*]

[a] *Department of Biochemistry, Chiang Mai University, 110 Inthawaroros Road., Sripoom, Muang, Chiang Mai, 50200, Thailand*
[b] *Department of Biology, Chiang Mai University, 239 Huaykaew Road, Suthep, Muang, Chiang Mai, 50200, Thailand*
[c] *Center of Excellence in Bioresources for Agriculture, Industry and Medicine, Chiang Mai University, Chiang Mai, 50200, Thailand*

ARTICLE INFO

Keywords:
Anticancer
Houttuynia cordata Thunb.
Hexane fraction
Extracts
Regulated apoptosis
Breast cancer

ABSTRACT

Houttuynia cordata Thunb. (HCT) is a perennial plant used in traditional Thai medicine for many centuries. This study aimed to investigate the antiproliferative effect of the hexane fraction, which has not been explored before. HCT ethanol extract (crude extract) was sequentially fractionated to obtain a hexane (H) fraction. GC-MS was used to determine the phytochemicals. The H fraction consisted of lipids, mainly α-linolenic acid and some terpenoids. MTT assay was used to determine the cytotoxic effects of H fraction in MCF-7, MDA-MB-231, NIH3T3 and PBMCs. The mode of cell death and cell cycle analysis were determined by flow cytometry. The mechanisms of cell death were defined by mitochondrial transmembrane potential (MTP) reduction and activation of caspase-3, -8 and -9. The expression levels of the Bcl-2 family, cell cycle-related, endoplasmic reticulum (ER) stress-associated proteins; and Akt/ERK signaling molecules were investigated by immunoblotting. The H fraction was toxic to MDA-MB-231 more than MCF-7 cells but not to NIH3T3 and PBMCs. The growth of MDA-MB-231 cells was inhibited through apoptosis. MTP was disrupted whereas caspase-3, -8 and -9 were activated. The expression of pro-apoptotic Bax and Bak was upregulated, while Bid and anti-apoptotic Bcl-xL proteins were downregulated. Cyclin D1 and CDK4 levels were downregulated. The cell cycle was arrested at G1. Moreover, GRP78 and CHOP elevation indicated ER stress-mediated pathway. The expression ratio of pAkt/Akt and pERK/ERK were reduced. Taken together, the molecular mechanisms of MDA-MB-231 cell apoptosis were via intrinsic/extrinsic pathways, cell cycle arrest, ER stress and abrogation of Akt/ERK survival pathways. According to the most current research, the H fraction may be used as an adjuvant in the BC treatment; however, before the anticancer strategy can be applied to patients, it is important to determine each active compound's effects in cell lines and *in vivo* when compared with a combined mixture.

1. Introduction

Data from GLOBOCAN 2020 revealed that breast cancer (BC) is the most common cancer occurring in females [1]. Moreover, BC

* Corresponding author.
E-mail address: ratana.b@cmu.ac.th (R. Banjerdpongchai).

https://doi.org/10.1016/j.heliyon.2023.e18755
Received 21 February 2022; Received in revised form 1 June 2023; Accepted 26 July 2023
Available online 28 July 2023

also occurs in men and transgender [2,3]. The heterogeneity of BC is explained by many parameters, such as tumor size, lymph node involvement, histopathology, grading or severity and age of cancer onset in BC patients. The biomarkers like estrogen receptor (ER), progesterone receptor (PR) and epidermal growth factor receptor 2 (HER2) are routinely used for diagnosis and implied for prognosis in BC patients [4]. BC can be grouped into estrogen receptor positive (ER+), e.g., MCF-7 and T47D and ER-negative, e.g., SKBR3, MDA-MB-231, MDA-MB-468 and MDA-MB-453. However, different molecular subtypes can be used to categorize BC, such as luminal A (ER + PR + HER2-), luminal B (ER + PR + HER2+), and basal-like HER2-positive ones [5,6]. The human MDA-MB-231 cell line is TNBC derived from the metastatic sites [7].

Plants contain phytochemicals that have been investigated in *in vitro* and *in vivo* models of efficiency for BC prevention [8]. Moreover, phytochemicals have played a significant role in BC treatment by increasing antioxidant enzyme expression, regulating cell signaling pathways and mediating apoptosis by causing cell cycle arrest, altering pro- and anti-apoptotic proteins expression and activating cell cycle arrest and caspases' activities [8]. Thai traditional medicine (TTM) has been widely used for centuries in Thailand, and it is essential to gain evidence-based research in cancer management to support the TTM practitioners' practice [9]. Thai patients frequently use TTM, which is popular for self-medication and as prescribed by TTM practitioners. However, their beneficial usage from such therapies is rarely monitored. The uncontrolled use of TTMs, many of which are uncharacterized, raised concerns; therefore, scientific research and validation of holistic medical regimes are urgently needed [10]. *Houttuynia cordata* Thunb. (HCT) is a member of Saururaceae, commonly distributed in Eastern and Southeast Asia [11]. It has been used as an edible vegetable and in traditional medicine including, TTM [9,10]. HCT has been consumed as food and either aqueous or ethanolic extracts or fermented ethanolic products that are produced as food supplements [12,13]. The latest study proved that HCT, whether taken as an extract or as a whole plant, has considerable medical advantages. HCT has been shown to have anti-leukemic, anti-cancer, anti-oxidative, anti-viral, anti-allergic, and anti-SAR activities in recent investigations on its pharmacological effects [14].

Our previous study reported that in human leukemia, the ethanolic extract of fermented HCT is cytotoxic to HL-60 >Molt- 4 > PBMCs, to a greater extent than the non-fermented preparation. The HCT ethanolic fermented extract can induce HL-60 and Molt-4 cell apoptosis via oxidative stress and the mitochondrial pathway [15]. HCT ethanolic extract shows antiproliferative effects on various cancer cell lines, including HeLa, HT29, HCT116, MCF-7and Jurkat; and induces cell cycle arrest [16,17]. We also have demonstrated that the certain fraction 4 from thin layer chromatography of HCT ethanolic extract reduces Bcl-xL and increases Smac/Diablo, Bax and GRP78 protein expression levels in Molt-4 cells, resulting in ER stress-mediated apoptosis [18]. Moreover, our groups also demonstrated that HCT ethanolic extract inhibits breast cancer MCF-7 and MDA-MB-231 cell growth, migration and invasion via G1 arrest, abolishes matrix metalloproteinases (MMPs) secretion and induces apoptosis via pro-apoptotic protein upregulation and caspase activation [19]. Apart from other fractions of HCT, the ethyl acetate (EA) fraction of HCT also suppresses the activation of MAPKs (p38 and JNK) signaling pathway [20]. However, the study of the H fraction of HCT remains poorly illustrated for its cytotoxicity on human BC cells. Hence, the current study aimed to investigate and compare the antiproliferative effects of HCT extract and various fractions towards human BC cells, determine the mode(s) of cell death, and the relevant molecular mechanisms in HCT H-treated cells. The MDA-MB-231 cell line possesses a highly invasive and poorly differentiated phenotype [7] that was used in this study. GC-MS was also utilized to determine the active components in the H fraction.

2. Materials and methods

2.1. Reagents and antibodies

The organic solvents (hexane, chloroform, ethyl acetate, methanol and acetic acid) were analytical grade and purchased from RCI Labscan Limited, Bangkok, Thailand. Dulbecco's Modified Eagle's Medium (DMEM), fetal bovine serum, streptomycin and penicillin G sodium were obtained from Gibco BRL (Thermo Fisher Scientific Inc., Waltham, MA, USA). Dimethyl sulfoxide (DMSO), 3-(4,5-dimethyl)-2,5-diphenyl tetrazolium bromide (MTT), propidium iodide (PI), Ficoll–Hypaque reagent (HISTOPAQUE®-1077) and 3,3′-dihexyloxacarbocyanine iodide ($DiOC_6$) were obtained from Sigma-Aldrich (St. Louis, MO, USA). Annexin V-FITC FLUOS kit (Cat No. 11858777 001) and protease inhibitor cocktail tablets (Cat No. 11697498001) were obtained from Roche Diagnostics, Mannheim, Germany. The substrates of caspase-9, LEHD-*para*-nitroaniline (LEHD-*p*-NA), caspase-8, (IETD-*p*-NA), caspase-3, (DEVD-*p*-NA) and RPMI-1640 medium were obtained from Invitrogen (Thermo Fisher Scientific Inc., Waltham, MA, USA). Primary antibodies against Bax (ab32503), Bak (ab69404), Bcl-xL (ab32370), Bid (ab2388), cyclin D1 (ab226977), CDK4 (ab137675), p21 (ab227443), Akt (ab32505), pAkt (Ser473) (ab81283), ERK (ab196883), pERK (ab76299), GRP78 (ab21685), DDIT3 (ab11419), β-actin (ab8227) and peroxidase-labeled secondary antibodies: goat anti-rabbit IgG (ab97051) and goat anti-mouse IgG linked to horseradish peroxidase (ab97023), were purchased from Abcam (Cambridge, UK).

2.2. Plant materials and extraction

Dried powder of *H. cordata* (Lot 05/2018) was obtained from the plant's aerial parts, which were generously provided by Prolac (Thailand) Co., Ltd., Lamphun Province, Thailand. For the taxonomic authentication, the whole plant of *H. cordata*, including roots, stems and leaves, was collected from the plantation bed of Prolac (Thailand) Co., Ltd., Lopburi Province, Thailand, in May 2018. Plant species were identified and authenticated by Dr. Narin Printarakul, a lecturer and senior plant taxonomist at the Department of Biology, Faculty of Science, Chiang Mai University, Chiang Mai, Thailand. The voucher specimen number is CMUB003997001, deposited in CMU Herbarium, Faculty of Science, Chiang Mai University, Chiang Mai, Thailand.

Sixty grams of powder were macerated in 1 L of 80% ethanol and refluxed at 70 °C overnight three times. The solution was filtered

through Whatman® filter paper No.1. The solvent was removed under vacuum by rotary evaporator, followed by evaporation at 95 °C to yield crude extract. The crude extract was re-dissolved in 3:7 of methanol-water and partitioned with various solvents in a ratio of 1:1 three times including, hexane (H), dichloromethane (DCM) and ethyl acetate (EA), respectively. For each fraction, the solvent was removed by a rotary evaporator. To avoid the cytotoxicity of hexane and other solvents, we completely removed all solvents by evaporation under a fume hood until the weight of extracts was constant. All fractions were kept at 4 °C until used.

2.3. Determination of total phenolic content

The total phenolic content was determined by a modified Folin-Ciocalteu colorimetric method [21]. Briefly, in a 96-well plate, five μL of each extract or fraction was mixed with 75 μL of deionized water, 20 μL of Folin-Ciocalteu reagent and neutralized with 100 μL of 7.5% Na_2CO_3 solution. After 30 min of incubation in the dark at room temperature, the plate was measured at 765 nm against blank using a microplate reader (BioTek, Winooski, Vermont, USA). The total phenolic content was calculated using an equation of a standard linear curve, with data expressed as mg of gallic acid equivalent (mg GAE) per gram of extract.

2.4. Screening of chemical components using gas chromatography-mass spectrometry (GC-MS)

GC-MS was used to analyze the H fraction at the Science and Technology Service Center (STSC-CMU), Faculty of Science, Chiang Mai University. The analysis was performed using GC 7890 Agilent Technology equipped with 5975C (EI) Agilent Technology (Santa Clara, CA, USA). The sample was separated on a DB5-MS column (30 m × 0.25 mm ID x 0.25 μm, Agilent). The following oven temperature program was used: an initial temperature of 50 °C, 3 min, a final temperature was 250 °C with 5 °C accelerating/min, with 43 min total run time. The injection was performed by a split mode with a split ratio of 1:1. Solvent delay time was 4 min. The mass scanning range was from 50 to 550 amu. The temperature was 150 °C for the MS quadrupole and 23 °C for the MS source.

2.5. Cell culture

The human breast cancer MDA-MB-231, MCF-7 and NIH3T3 murine embryonic fibroblast cells were obtained from the American Type Culture Collection (ATCC, Manassas, VA, USA). Cell lines were cultured in Dulbecco's Modified Eagle Medium (DMEM) with 25 mM $NaHCO_3$, 100 units/mL penicillin, 100 μg/mL streptomycin and supplemented with 10% inactivated fetal bovine serum. The cells were incubated at 37 °C under 5% CO_2 atmosphere. The cells were passaged not more than 5–6 passages and cultured until 80–90% confluency before treatment.

Peripheral blood mononuclear cells (PBMCs) were obtained from the Blood Bank Unit of Maharaj Nakorn Chiang Mai Hospital, Faculty of Medicine, Chiang Mai University, Thailand. It was initially provided as packed red cells from the donated blood from the Blood Bank Unit of Maharaj Nakorn Chiang Mai Hospital, affiliated to the Faculty of Medicine, Chiang Mai University, Chiang Mai, Thailand. Human PBMCs' experiments were approved by the Institutional Review Board and the Research Ethical Committee at the Faculty of Medicine, Chiang Mai University, Chiang Mai, Thailand (No. EXEMPTION: REC-25610515-13791, approved on June 5, 2018).

The healthy donors of the PBMCs used in this study were based on the criteria of the Blood Bank Unit at Maharaj Nakorn Chiang Mai Hospital, Faculty of Medicine, Chiang Mai University, Chiang Mai, Thailand. The characteristics of the donors include general healthy, without risks of sexual behaviors to exclude HIV infection or sexually transmitted diseases and conditions that might increase infection risks, such as Hepatitis B, and C virus infection; and a history of drug intake. The age range of donors is between 18 and 60 years old for both genders. The volunteer must not have a history of chronic diseases, for example, diabetes, cancer, hematological disorders, hypertension, renal and liver diseases. The hemoglobin range in males' is between 13.0 and 18.5 g/dL, for females', is 12.5–16.5 g/dL. Systolic blood pressure must not be more than 160 mmHg, whereas diastolic blood pressure must not be more than 100 mmHg. The pulse rate range must be between 50 and 100 per minute. The volunteers' weight must be over 50 kg. All volunteers' information was confidential. The consent form must be agreed upon and signed by every volunteer.

2.6. Cytotoxicity assay by MTT

MCF-7, MDA-MB-231, NIH3T3 and PBMCs were treated with crude extract, methanol fraction, ethyl acetate (EA) fraction, dichloromethane (DCM) fraction and hexane (H) fraction at various concentrations in serial dilution, such as 50, 100, 150, 200, 300, 400 μg/mL. After 24 h of incubation with each extract and fractions, the cells were added with MTT dye and incubated at 37 °C for 4 h. The formazan crystal was dissolved in DMSO, and the absorbance was measured at 540 nm and a reference wavelength at 630 nm using a microplate reader (BioTek, Winooski, VT, USA). The following formula was used to calculate the percentage of cell viability [22]. The inhibitory concentrations at 20% (IC_{20}) and 50% (IC_{50}) were calculated and employed for further experiments to examine the dose-response manner.

Percentage of cell viability = [Mean absorbance in treated wells/Mean absorbance in control wells] x 100

2.7. Mode of cell death determination by flow cytometry

Cancer cells (5×10^5 cells/well in a 24-well culture plate) were treated at IC_0, IC_{20} and IC_{50} concentrations. After incubation at 37 °C under a 5% CO_2 atmosphere for 24 h, the cells were washed twice with phosphate-buffered saline (PBS) and centrifuged. Next, the cells were resuspended and stained with 100 μL of binding buffer containing five μL of annexin V-fluorescein isothiocyanate (FITC) and propidium iodide (PI) (Roche Diagnostics, Mannheim, Germany) for 15 min in the dark. The fluorescence intensity of the cells was measured. The dot plot character of the cells was processed using a flow cytometer (Beckman Coulter, IN, USA). The percentage of viable and apoptotic cells was calculated [23].

2.8. Measurement of caspase-3, -8 and -9 activities

Cancer cells (1.5×10^6 cells/well in a 6-well culture plate) were incubated with IC_0, IC_{20} and IC_{50} concentrations for 24 h. The cells were collected and lysed in a lysis buffer for 15 min on ice. The colorimetric protease assay kit (Invitrogen, Thermo Fisher Scientific Inc., MA, USA) was used to determine the caspase activities: caspase-3 substrate, DEVD- *p*-NA; caspase-8 substrate, IETD- *p*-NA; and caspase-9 substrate, LEHD- *p*-NA, as described in a previous study. the optical density at 405 nm was measured by a spectrophotometric microplate reader (BioTek, Winooski, VT, USA) [24].

2.9. Determination of mitochondrial transmembrane potential (MTP, $\Delta\psi m$)

Cancer cells (5×10^5 cells/well in a 24-well culture plate) were treated with IC_0, IC_{20} and IC_{50} concentrations for indicated times (12 and 24 h). After incubation, cells were harvested and re-suspended in PBS. Then $DiOC_6$ (Sigma-Aldrich, St. Louis, MO, USA) was added to the final concentration at 40 nM, and the cells were further incubated for 15 min at 37 °C. The reduction of mitochondrial transmembrane potential was determined by a flow cytometer (Beckman Coulter, IN, USA) [18].

2.10. Cell cycle analysis

Briefly, cancer cells (1.5×10^6 cells/well in a 6-well culture plate) were incubated at IC_0, IC_{20} and IC_{50} concentrations for 24 h. Cells were stained with PI, cell cycle distribution as histograms and the percentages of cells in G0/G1, S and G2/M phases were analyzed by a flow cytometer (Beckman Coulter, IN, USA) [17].

2.11. Determination of apoptosis-related/cell cycle regulating and survival pathway-associated protein expression by Western blotting

After cancer cell treatment at IC_0, IC_{20} and IC_{50} concentrations, the collected cells were lysed with a RIPA buffer containing protease inhibitor (Roche, Mannheim, Germany). The protein concentration of each sample was measured by Bradford assay kit (Thermo Fisher Scientific, Waltham, MA, USA). As in the previous system, Western blot analysis was used to determine protein expression levels [19]. The membrane was then incubated with primary antibodies against individual protein such as apoptotic Bcl-2 related proteins (Bax, Bak, Bcl-xL and Bid); cell cycle regulating proteins (cyclin D1, CDK4 and p21); survival signaling molecules (Akt, pAkt, ERK and pERK); ER stress proteins (GRP78 and DDIT3) and β-actin at 4 °C overnight. Then the membrane was washed in appropriate conditions to remove excess and non-specific binding antibodies. Afterward, it was incubated with horseradish peroxidase (HRP)-conjugated secondary antibodies at room temperature. Finally, the protein-antibody complex was detected using enhanced chemiluminescence (ECL) SuperSignal® protein detection kit (Thermo Fisher Scientific, Waltham, MA, USA). The band densities were measured by ImageJ (National Institute of Health, Bethesda, MD, USA).

2.12. Statistical analysis

Data were presented as mean ± standard deviation (S.D.) from triplicates of three independent experiments. All tests were administered using commercially available software, namely, GraphPad Prism 6.0 software (GraphPad Software, Inc., San Diego, CA, USA). The data were assessed with one-way analysis of variance (ANOVA) using post hoc Tukey's test. Comparisons between the two unpaired groups were evaluated using unpaired or independent Student's *t*-test. The standard linear graph of Fig. S1 was analyzed by multiple linear regression. Data were considered significant when p value < 0.05.

3. Results

3.1. Alpha-linolenic acid as the main components in hexane fraction of H. cordata

The weight and percentage yield of each fraction from 60 g of *H. cordata* dried powder was as follows: crude extract (11.2 g, 18.67%), hexane (0.8 g, 1.33%), ethyl acetate (3.4 g, 5.67%) and dichloromethane (1.8 g, 3.0%) fractions (Table S1). The total phenolic content in each fraction was determined and shown as gallic acid equivalence (GAE) (Table S2). The gallic acid in various concentrations was used as standard in 80% MeOH, and its linear regression equation was shown in Fig. S1. The result of the GC-MS chromatogram of the H fraction is shown in Fig. 1 and Table 1. The major components found in HCT H fraction were lipids (α-linolenic acid (ALA) 42.76%, palmitic acid 15.49% and 9,12,15-octadecatrienoic acid ethyl ester 9.38%). Almost all the minor compounds were

in the group of terpenoids such as phytol (5.76%), dodecanoic acid (2.22%), neophytadiene (0.64%), isophytol (0.56%), cyclopentanol (0.39%) and eicosane (0.13%). In our study, we also found various phenolic acids and a few flavonoids in the ethanolic extract and each fraction using the HPLC technique.

3.2. *H. cordata H fraction-induced breast cancer cytotoxicity*

Based on the mitochondrial enzyme NAD(P)H-dependent oxidoreductase, which converts MTT to insoluble purple formazan crystal, metabolic activity indicates cell viability [25]. MTT assay was used to confirm the effect of crude extract and three fractions of HCT (hexane, ethyl acetate and dichloromethane fractions) on human BC cell lines (MCF-7 and MDA-MB-231) compared with normal murine fibroblast NIH3T3 cells and PBMCs.

After incubation for 24 h, the percentages of cell viability and the 50% inhibitory concentrations (IC_{50} value) on MDA-MB-231 and MCF-7 together with normal NIH3T3 and PBMC cells are shown in Fig. 2 and Table 2, respectively. The crude extract at 24 h demonstrated inhibitory concentrations on MDA-MB-231 ($IC_{50} = 156.90 \pm 8.58$ μg/mL) and MCF-7 cells ($IC_{50} = 174.03 \pm 1.88$ μg/mL). The selectivity index (SI), the ratio between IC_{50} of individual normal PBMCs or NIH3T3 cells and IC_{50} of each cancer cell type at 24 h of treatment, are shown in Table 3. The percentages of cell viability and IC_{50} of MDA-MB-231 and MCF-7 treated by H fraction accounted for 289.53 μg/mL and 337.73 μg/mL, respectively (Fig. 2B and Table 2). H fraction significantly decreased the cell viability in a concentration-dependent manner (Fig. 2B). The IC_{50} value indicated that MDA-MB-231 cells were more sensitive to crude extract and H fraction than MCF-7 cells. Therefore, we selected the most sensitive breast cancer cell line when compared to the other BC cell as same as in our previous studies presenting the cholangiocarcinoma cancer cells' model [26] and the MDA-MB-231 when compared to less sensitive cells or normal epithelial mammary MCF10A cells [27]. MDA-MB-231 cells were then chosen for further investigating the mode and mechanisms of cell death induced by HCT H fraction.

Cancer and normal cells: NIH3T3 (an adherent cell) and PBMC (a suspending cell); were used to compare the sensitivity of HCT crude extract and fractions. The crude extract, hexane and ethyl acetate fractions were nontoxic to NIH3T3 cells at a concentration of 400 μg/mL. However, the dichloromethane fraction was found to be harmful against NIH3T3 cells at concentrations greater than 100 μg/mL ($IC_{50} = 176.07 \pm 9.94$ μg/mL) when cultured for 24 h. It was demonstrated that neither crude extract nor H fraction was harmful to PBMCs at a maximum concentration of 400 μg/mL for 24 h of incubation. In Fig. 2A and B, they showed the dose-response manner of human BC MCF-7 and MDA-MB-231 cytotoxicity when the cells were treated with crude extract and H fraction.

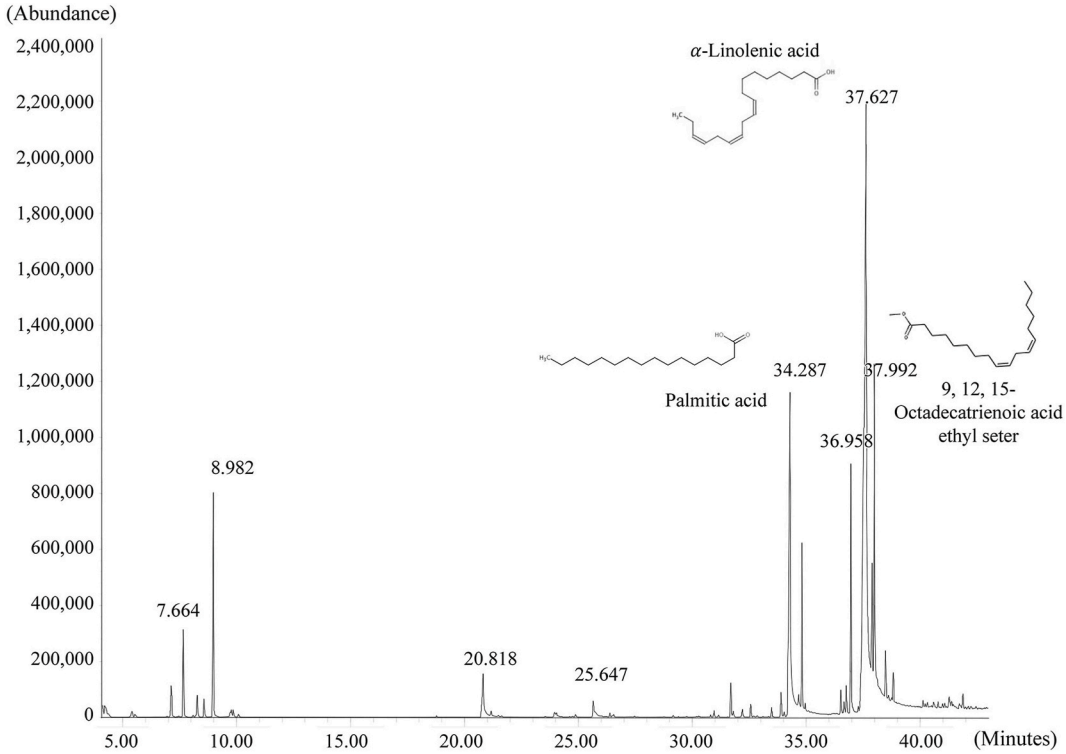

Fig. 1. The GC-MS chromatogram of bioactive compounds in the H fraction of *H. cordata*. The HCT H fraction was analyzed using GC-MS instrument GC 7890 Agilent Technology equipped with 5975C (EI) Agilent Technology. The sample was separated on a DB5-MS column (30 m × 0.25 mm ID x 0.25 μm, Agilent). The chemical structures of three major compounds are presented.

Table 1
The GC-MS profile of HCT-H fraction.

Peak number	Retention time	Peak area (%)	Name of the compound
1	4.213	0.45	Cyclopentanol
2	7.131	0.84	Unknown
3	7.663	2.03	Unknown
4	8.275	0.56	Unknown
5	8.573	0.41	Unknown
6	8.979	4.69	Unknown
7	20.818	1.90	Capric acid
8	25.653	0.28	Dodecanoic acid
9	31.690	0.67	Neophytadiene
10	32.193	0.17	Unknown
11	32.565	0.27	Neophytadiene
12	33.486	0.19	Palmitic acid
13	33.893	0.48	Isophytol
14	34.287	15.49	Palmitic acid
15	34.671	0.78	Vaccenic acid
16	34.820	3.56	Palmitic acid ethyl ester
17	34.957	0.19	Eicosane
18	36.525	0.54	Cyclohexadecane
19	36.662	0.31	9,12-Octadecadienic acid
20	36.765	0.67	9,12,15-Octadecatrienoic acid
21	36.960	5.27	Phytol isomer
22	37.629	42.76	α-Linolenic acid
23	37.887	4.06	Linoleic acid ethyl ester
24	37.995	9.38	9,12,15-Octadecatrienoic acid ethyl ester
25	38.115	1.47	Stearic acid
26	38.493	1.37	Stearic acid ethyl ester
27	38.825	0.69	Neophytadiene
28	41.274	0.24	9-Octadecenamide
29	41.869	0.29	Ethyl icosanoate (Eicosanoic acid ethyl ester)

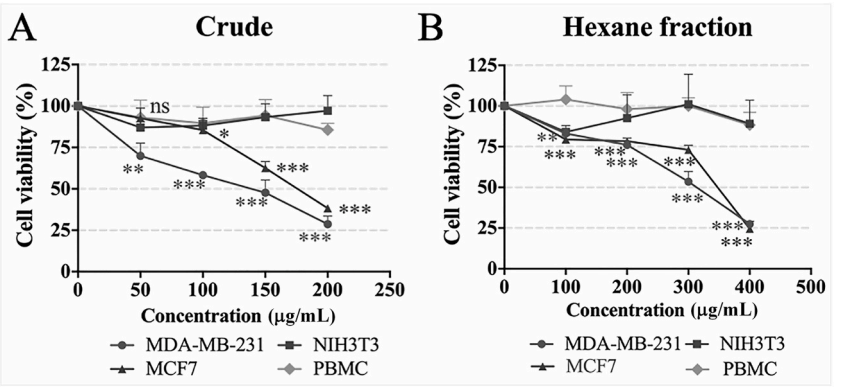

Fig. 2. Cytotoxicity of *H. cordata* crude extract and H fraction against human breast cancer MDA-MB-231 and MCF-7 cell lines, normal murine embryonic fibroblast NIH3T3 cell line, and human peripheral blood mononuclear cells (PBMCs). The percentage cell viability of these cells is shown on the Y-axis. The percentage of cell viability was determined after treatment with crude extract (A), and hexane fraction (B) for 24 h at various concentrations as shown on the X-axis. The data are reported as mean ± S.D. of triplicate from three independent experiments. The significance of statistical values is marked with $*p < 0.05$, $**p < 0.01$, $***p < 0.001$ vs control.

Table 2
Summary of the 50% inhibitory concentration (IC_{50}) of crude extract and each fraction on MDA-MB-231, MCF-7, NIH3T3 cells, and PBMCs.

Extract/fractions	IC_{50} (µg/mL) at 24 h			
	MDA-MB-231	MCF-7	NIH3T3	PBMC
Crude	156.90 ± 8.58	174.03 ± 1.88	>400	>400
Hexane	289.53 ± 9.03	337.73 ± 2.40	>400	>400
Ethyl acetate	297.67 ± 18.22	80.63 ± 3.21	>400	>400
Dichloromethane	155.80 ± 8.41	126.50 ± 19.08	176.07 ± 9.94	>400

Table 3
Selectivity index (SI) of HCT H fraction in BC cells compared to normal cells.

Cell lines	SI (compared to NIH3T3)	SI (compared to PBMCs)
MDA-MB-231	>2.25	>1.43
MCF-7	>1.93	>1.23

Note: Selectivity index (SI) is the ratio between IC_{50} values of normal NIH3T3 cells or PBMCs and the IC_{50} value of each BC cell.

3.3. Apoptosis induction in HCT H fraction-treated-MDA-MB-231 cells

Induction of cancer cell apoptosis is a potential mechanism to reduce cancer cell growth [28]. Phosphatidylserine externalization is a characteristic of apoptotic cells [29,30]. Dot plot analyses showed the increased percentage of early apoptosis (lower right quadrant) and late apoptosis cells (upper right quadrant) at IC_{20}, IC_{50} (189.7 and 289.5 μg/mL) using positive control of 5 μM navelbine (a conventional chemotherapeutic drug) (Fig. 3A). The percentage of early apoptotic cells at IC_{20} and IC_{50} significantly increased dose-dependently (Fig. 3B).

3.4. Reduction of mitochondrial transmembrane potential (MTP) in H fraction-treated MDA-MB-231 cells

MTP is crucial for maintaining the function of the respiratory chain and ATP generation. When the electrochemical gradient across the mitochondrial membrane collapses, the alteration in mitochondrial permeability is an important phenomenon that leads to apoptosis induction [31]. The histograms of MDA-MB-231 cells treated with H fraction at IC_{20}, and IC_{50} (189.7 and 289.5 μg/mL) for 12 h (Fig. 4A) and 24 h (Fig. 4B) demonstrated that the fluorescence signal of $DiOC_6$ fluorochrome was reduced due to the disruption of MTP. The percentage of cells with the loss of MTP increased in a dose-response manner. Bar graphs exhibited the increased percentage of cells with MTP loss at 12, and 24 h of H fraction exposure significantly at both concentrations. When the two-time durations were compared, the percentage of cells with MTP loss also enhanced in both dose- and time-dependent manners (Fig. 4C).

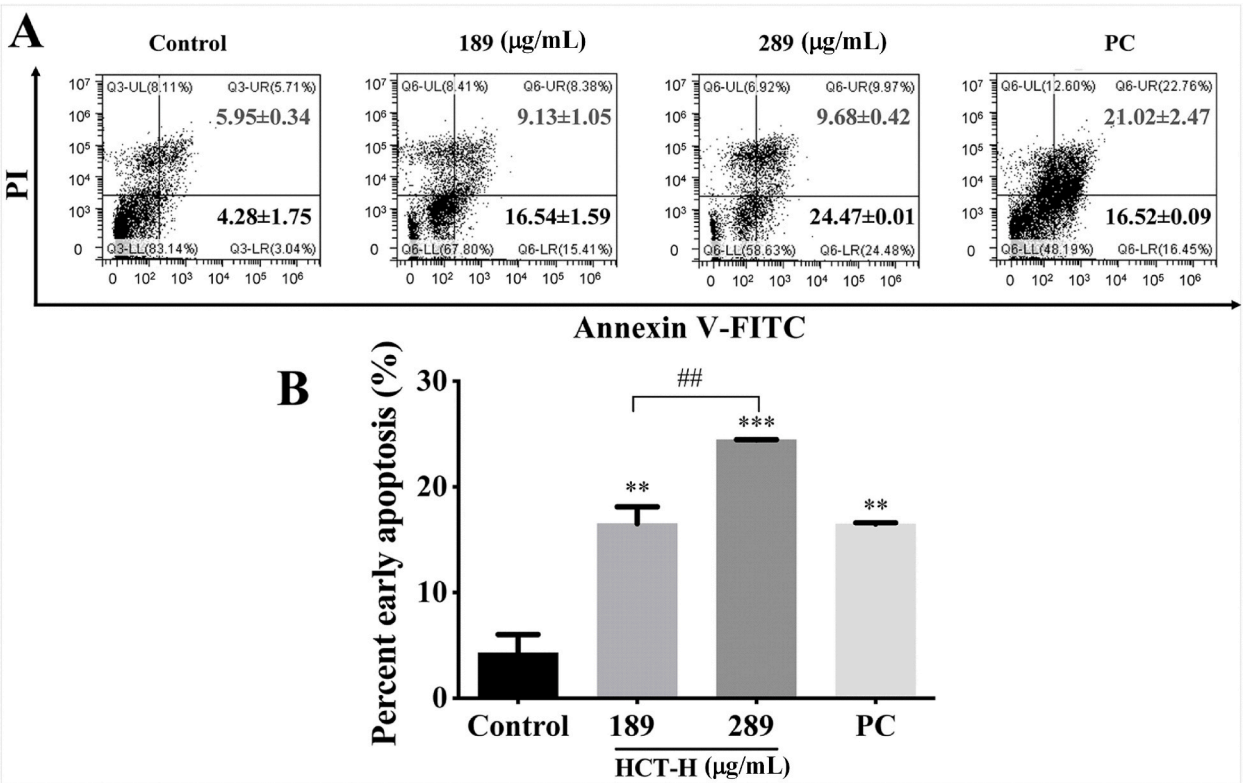

Fig. 3. Apoptosis in MDA-MB-231 cells induced by HCT H fraction. Dot plot analysis of MDA-MB-231 cells treated with different concentrations of H fraction at 0, 189, and 289 μg/mL, and Navelbine 5 μM as a positive control for 24 h (A). The bar graphs show the percentage of early apoptosis (B). The data are reported as mean ± S.D. of three independent experiments. The significance of statistical values is marked with $^{**}p < 0.01$, $^{***}p <$ 0.001 vs control. The comparison between groups is marked with $^{\#\#}p < 0.01$.

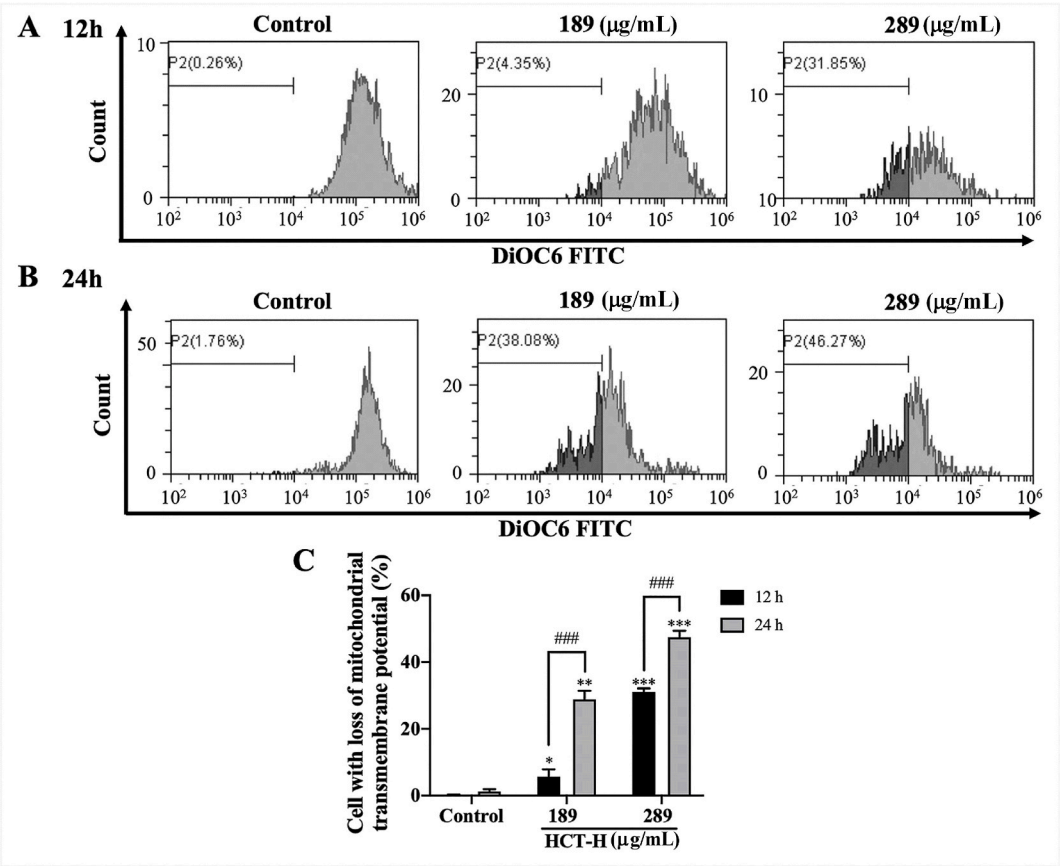

Fig. 4. Reduction of mitochondrial transmembrane potential (MTP) of HCT H fraction-treated MDA-MB-231 cells. The cells were treated with HCT H fraction at 0, 189, and 289 μg/mL, then stained with $DiOC_6$ (3,3′ dihexyloxacarbocyanine iodide) and the fluorescence was measured by employing flow cytometry technique. The histograms show the MTP of MDA-MB-231 cells after treatment with fraction at 0, 189, and 289 μg/mL, for 12 h (A) and 24 h (B). The bar graphs show the percentage of cells with loss of MTP compared between 12 h (black bars) and 24 h (grey bars) (C). The data are reported as mean ± S.D. for the three independent experiments. The significance of statistical values is marked with $^{*}p < 0.05$, $^{**}p < 0.01$, $^{***}p < 0.001$ vs control. The comparison between groups is marked with $^{\#\#\#}p < 0.001$.

3.5. Induction of caspase-3, -8 and -9 activities in H fraction treated-MDA-MB-231 cells

From the previous experiments, MTP disruption is one of the hallmarks of apoptosis [31]. Apoptosis is primarily implemented by a family of cysteinyl aspartate-specific proteases or caspases [28,32]. The mechanism of apoptosis is mainly controlled by caspases acting as both initiators and executioners [33]. Caspases' activities can be applied to indicate the different apoptotic cell death

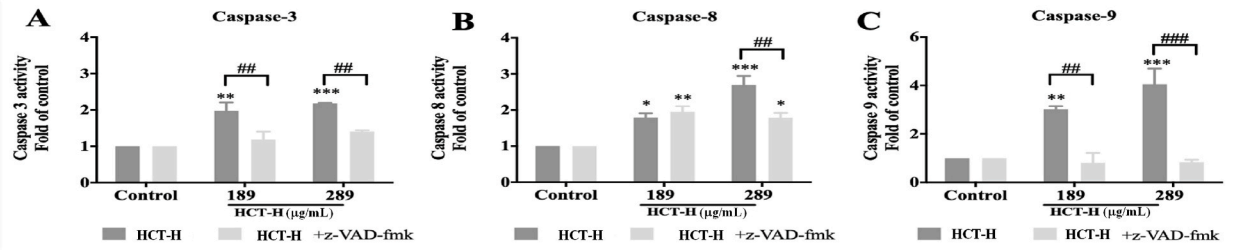

Fig. 5. The induction of caspase-3, -8 and -9 activities in MDA-MB-231 cells after treatment with HCT H fraction at 0, 189, and 289 μg/mL, for 24 h in the status without or with 10 μM z-VAD-fmk (a pan-caspase inhibitor) prior treatment for an hour. The bar graphs show the activity of each caspase compared to the control in fold(s) of activity. Caspase-3 (A), caspase-8 (B) and caspase-9 (C) activities are exhibited, respectively. The black bars are caspase activity without z-VAD-fmk, whereas the grey bars are with z-VAD-fmk prior treatment. The data are reported as mean ± S.D. of triplicate from three independent experiments. The significance of statistical values is marked with $^{*}p < 0.05$, $^{**}p < 0.01$, $^{***}p < 0.001$ vs control. The comparison between groups is marked with, $^{\#\#}p < 0.01$, $^{\#\#\#}p < 0.001$.

pathways, viz., intrinsic, extrinsic and ER stress pathways [34,35]. The activities of caspase-3 (Fig. 5A), −8 (Fig. 5B) and −9 (Fig. 5C) increased after H fraction treatment for 24 h in a dose dependent manner. Additionally, the induction of caspase-3, -8 and -9 activities was reduced when MDA-MB-231 cells were pretreated with the pan-caspase inhibitor (z-VAD-fmk) for an hour before HCT H fraction incubation.

3.6. Cell cycle arrest at G1 and alteration of apoptosis-related/cell cycle regulatory protein levels in H fraction-treated MDA-MB-231 cells

The balance between the pro-apoptotic and anti-apoptotic proteins in the Bcl-2 family is predominant in defining whether a cell encounters apoptosis [32]. Activation of pro-apoptotic proteins counteracts the anti-apoptotic proteins leading to disruption of mitochondrial outer membrane permeability (MOMP) and release of various kinds of mitochondrial proteins, such as cytochrome *c*, into the cytosol [36]. HCT H fraction-treated MDA-MB-231 cells efficaciously promoted apoptotic cell death, while the expression levels of Bax and Bak, multi-domain pro-apoptotic proteins, were significantly elevated at IC_{50}, viz., 289.5 μg/mL (Fig. 6A–C). The anti-apoptotic protein Bcl-xL was majorly downregulated in a concentration-dependent manner (Fig. 6D). The expression of Bid was cleaved by active caspase-8 and significantly downregulated at 289.5 μg/mL (Fig. 6E).

The inhibitory effects of HCT H fraction on MDA-MB-231 cell growth and cell cycle progression have not been studied before. Firstly, the flow cytometric assay of the cell cycle distribution was investigated and exhibited that H fraction at IC_{50} (289.5 μg/mL) increased the cell population at the G1 phase, accounting for a mere 2% more than the control (Fig. 7A and B). To confirm that HCT H fraction induced anti-proliferation through cell cycle arrest, the expression of the G1 transition cell cycle checkpoint-regulated proteins such as CDK4 and cyclin D1 [37,38] were investigated by immunoblotting. It was demonstrated that the CDK4 and cyclin D1 protein expression levels were reduced, indicating cell cycle arrest at the G1 phase (Fig. 7C–E).

3.7. HCT H fraction-induced ER stress mediated-apoptosis in MDA-MB-231 cells

One of the unfolded protein response (UPR) downstream effectors, the transcription factor C/EBP homologous protein (CHOP) or DNA damage-inducible transcript 3 (DDIT3) or Growth arrest and DNA damage gene 153 (Gadd153) inhibits Bcl-2 family proteins and causes growth arrest and induces DNA damage and therefore promotes apoptosis [39,40]. The present study exhibited that the ER stress protein bands (Fig. 8A), cytosolic GRP78 expression level was increased (Fig. 8B), along with the raised CHOP expression level (Fig. 8C), indicating the ER stress pathway associated with HCT H fraction-induced MDA-MB-231 regulated apoptosis.

3.8. Attenuation of Akt and ERK pro-survival signaling pathways in HCT H fraction-treated MDA-MB-231 cells

The hallmarks of cancer include the capability to sustain proliferative signaling and resist cell death [41,42]. The cell pro-survival signaling proteins such as Akt and ERK and their phosphorylated forms (pAkt and pERK) are also inversely related to apoptotic cell death, namely in negatively regulated cell death signaling [43–45]. We performed immunoblotting to examine whether the H fraction repressed a cell survival signaling pathway. Both pAkt/Akt and pERK/ERK protein expression levels were significantly downregulated,

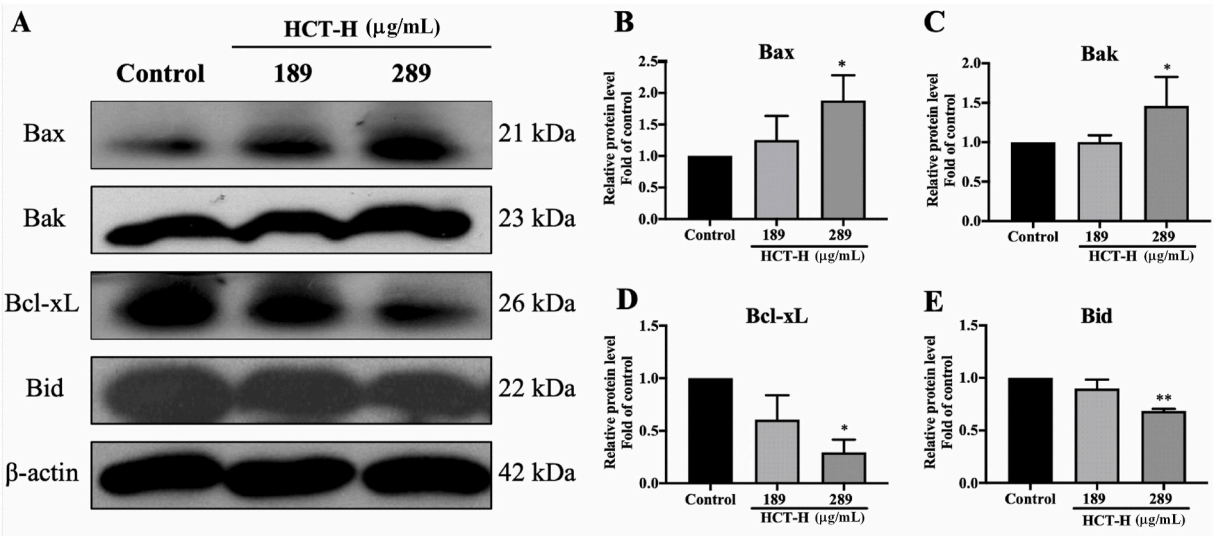

Fig. 6. The effects of HCT H fraction on the expression of apoptotic-involving proteins. MDA-MB-231 cells were treated with H fraction at 0, 189, and 289 μg/mL, for 24 h. The whole lysates were prepared and subjected to Western blotting to determine the protein expression levels of Bax, Bak, Bcl-xL, and Bid (A). The bar graphs represent the mean ± S.D. of band density of Bax (B), Bak (C), Bcl-xL (D), and Bid (E) using β-actin as the loading control. The data are reported from three independent experiments. The significance of statistical values is marked with $*p < 0.05$, $**p < 0.01$.

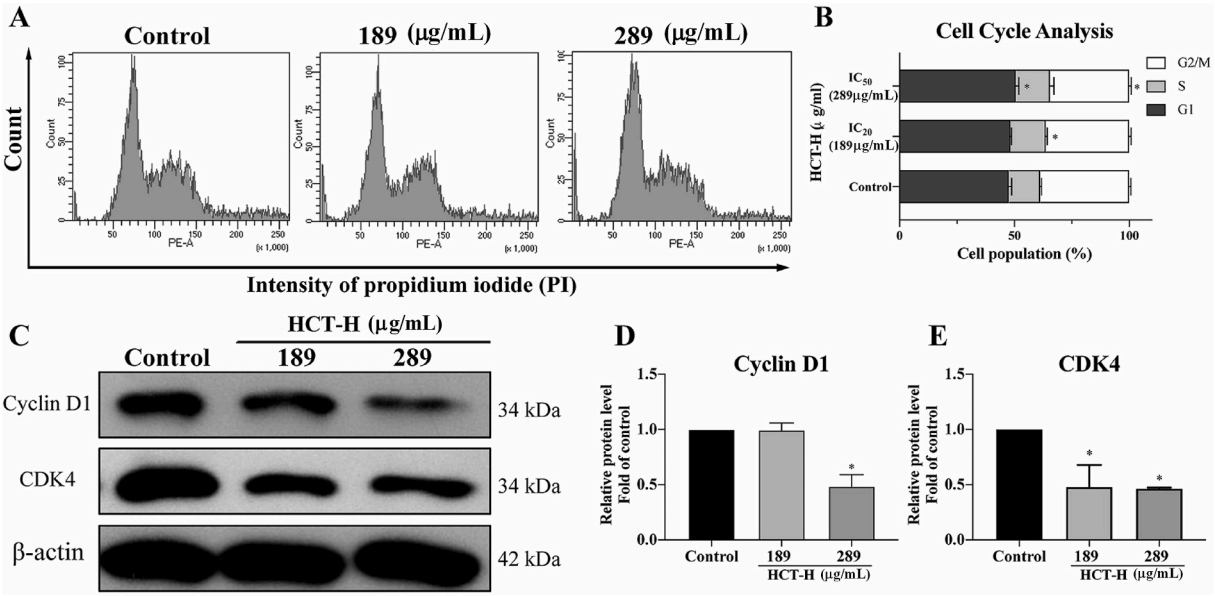

Fig. 7. The inhibitory effect on cell cycle-regulated protein expression levels in *H. cordata* H fraction-treated MDA-MB-231 cells. Cell cycle analysis of MDA-MB-231 cells treated with different concentrations of H fraction at 0, 189, and 289 μg/mL, for 24 h by flow cytometry (A). The bar graphs show the percentage of cells in each phase of the cell cycle (B). The whole lysates were prepared and subjected to Western blotting and the protein bands were shown in (C). The bar graphs are illustrated as the mean ± S.D. of the band density of cyclin D1 (D) and CDK4 (E) using β-actin as the loading control. The data are reported from three independent experiments. The significance of statistical values is marked with $^{*}p < 0.05$.

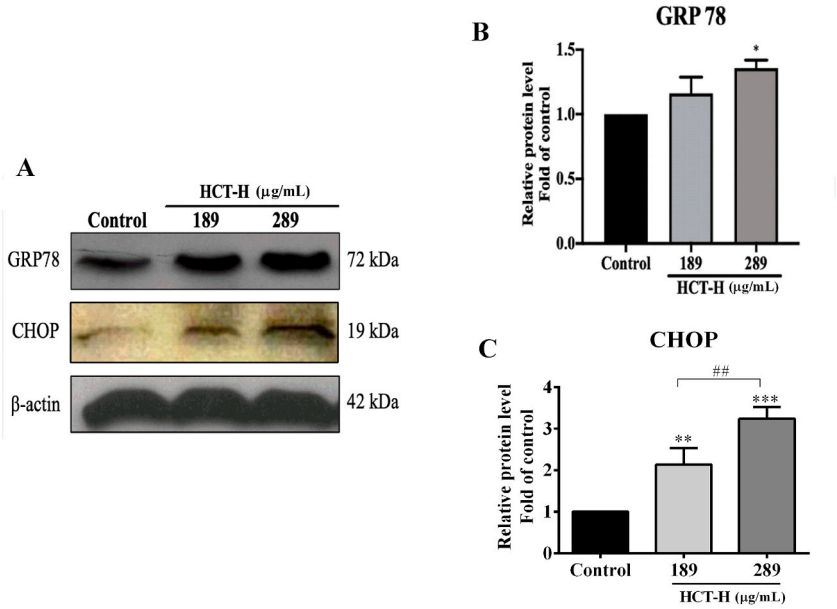

Fig. 8. Alteration of ER stress-related protein expression levels in H extract treated-MDA-MB-231 cells. MDA-MB-231 cells were incubated with HCT H fraction at 0, 189, and 289 μg/mL, for 24 h. The whole lysates were prepared and subjected to Western blotting (A). The bar graphs illustrated the mean ± S.D. of the band density of GRP78 (B) and CHOP (C) using β-actin as the loading control. The data are reported from three independent experiments. The significance of statistical values is marked with $^{*}p < 0.05$, $^{**}p < 0.01$ and $^{***}p < 0.001$ vs control. The comparison between groups is marked with $^{\#\#}p < 0.01$.

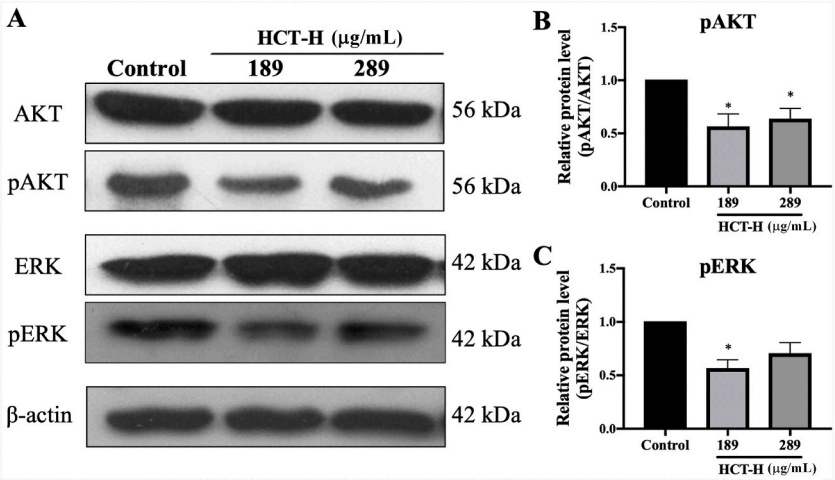

Fig. 9. The protein expression levels of pro-survival pAkt/Akt and pERK/ERK pathway after MDA-MB-231 treatment with HCT H fraction. MDA-MB-231 cells were treated with H fraction at 0, 189, and 289 μg/mL, for 24 h. The whole lysates were prepared and subjected to immunoblotting and the protein bands are demonstrated (A). The bar graphs illustrated the mean ± S.D. of the band density of pAkt/Akt (B) and pERK/ERK (C) using β-actin as the loading control. The data are reported from three independent experiments. The significance of statistical values is marked with * $p < 0.05$ vs control.

as shown in Fig. 9A–C.

4. Discussion

The HCT H fraction was evaluated in this study as a novel fraction for prospective BC therapy. It was more cytotoxic to MDA-MB-231 breast cancer cells than to MCF-7 but not to normal murine fibroblast NIH3T3 cells or human PBMCs. According to our previous studies, we used NIH3T3 as a control for MDA-MB-231 cells [46]. We also used PBMCs as another type of control for testing the cytotoxicity of the HCT H fraction to compare with BC cells. Several studies conducted to determine the biological effects of HCT extract and fractions. Many reports claim that HCT ethanolic extract has anti-BC effects. Houttuyninum, a phytochemical in HCT, inhibits HER2 phosphorylation in MDA-MB-453 (TNBC) cells dose-dependently by preventing the downstream components ERK1/2 and Akt activation [47]. HCT ethanolic extract also lessens cell migration and invasion in MDA-MB-231 and MCF-7. In addition, BC cells exposed to high doses of HCT ethanolic extract exhibit the activation of apoptosis. Moreover, HCT ethanolic extract increases caspase activity and enhances caspase and pro-apoptotic Bcl-2 family protein expression [19]. In the recent date, the topical administration of ethanol HCT extract model enhances the ratio of CD8+/Treg cells entering tumors and suppresses the growth of cutaneous squamous cell carcinoma (SCC) [48]. HCT ethyl acetate (EA) fraction induces apoptosis in androgen-sensitive prostate cancer cells (LNCaP) and castration-resistant prostate cancer (CRPC) (PCai1) cells by caspases activation, down-regulation of androgen receptors, and inactivation of Akt/ERK/MAPK signaling [49]. Another report found that HCT EA enhances HIF-1A–FOXO3 and MEF2A pathways and induces human HepG2 hepatocellular carcinoma cell apoptosis [50]. Besides, HCT EA represses the NF-κB and MAPK signaling pathways in RAW 264.7 macrophages, which prevents the release of pro-inflammatory mediators [20]. Additionally, HCT chloroform (CHL) and hexane fraction exhibit anti-oxidant effects as weak radical scavengers in ABTS and DPPH models [14]. Additionally, HCT butanol fraction increases the mRNA expression of apoptosis-mediated signaling molecules and reduces the proliferation of the BGC-823 gastric cancer cell [51]. Recently, molecular docking techniques were used to validate the active HCT components and they demonstrated a high affinity for binding to core targets. Through the TNF and PI3K/Akt signaling pathways, these findings suggested a potential pharmacological effect on radiation-induced lung injury (RILI), the most prevalent and serious side effect of radiation therapy for lung cancer and breast cancers [52]. Besides, using an in-silico docking technique, the top-hit phytochemicals from HCT were discovered to be potential inhibitors for the overexpressed cancer genes HER2 (breast) and VEGFR2 (stomach). The highest binding affinities to the HER2 and VEGFR2 receptors are exhibited by β-sitosterol and quercetin, which do so through both hydrogen and hydrophobic contacts [53]. *In vitro* studies have shown that sodium new houttuyfonate (SNH), a derivative of an HCT component, significantly reduces the proliferation, migration, and invasiveness of human MCF-7 and canine CMT-1211 breast cancer cells and promotes apoptosis. SNH increases the production of unchecked ROS, which leads to mitochondrial dysfunction. The PDK1-AKT-GSK3 pathway is then deactivated by SNH, which induces apoptosis [54]. Being a flexible plant, HCT has a wide range of potential uses in the treatment of many diseases, including in the forms of extracts and derivatives. More in-depth investigation is still needed to determine the full therapeutic potential and molecular mechanisms of action of each of these isolates, both individually and collectively, for greater treatment effectiveness [55].

In this study, the major compounds in the HCT H fraction were α-linolenic acid (ALA), palmitic acid and 9,12,15-octadecatrienoic acid ethyl ester, respectively, whereas the minor constituents were terpenoids. ALA is an omega-3 fatty acid, a necessary polyunsaturated fatty acid (PUFA) for humans with anti-inflammatory properties [56]. Additionally, both ALA and DHA can inhibit BC cell

growth via the HER2 signaling pathway [57]. Regardless of receptor subtype expression, ALA inhibits cell growth and causes apoptosis in MCF-7 (ER+/PR+/HER2-) and MDA-MB-231 (ER-/PR-/HER2- or TNBC) cells [58]. ALA also inhibits MCF-7 and MDA-MB-231 cell proliferation through the regulation of NO release, induction of lipid peroxidation, activation of caspase-3 and induction of mitochondrial apoptosis pathway [59]. The essential oils of HCT consist of 346 volatile components, mainly terpenoids [11]. Terpenoids are the diverse classes of plant secondary metabolites used and applied in pharmaceutical and industrial sections [60]. Terpenoids possess anticancer action in ovarian and breast cancers [61,62]. The mechanisms of action against BC include inhibition of cell proliferation and migration; activation of apoptosis; angiogenesis and metastatic suppression, both *in vitro* and *in vivo* [61]. For example, triterpenoids such as ursolic acid (UA) and oleanolic acid (OA) from the fraction F4 (subsequent hexane fractions) of *Wrightia tomentosa* Roem. & Schult. inhibit MCF-7 and MDA-MB-231 cell proliferation through G1 cell cycle arrest and induce apoptosis [63,64]. Thus, UA and OA are potential phytochemicals for BC therapeutics [8,64]. Moreover, two important phytochemicals that have been isolated from *H. cordata* and are used as anthelmintics by the Naga tribes of northeastern India are betulinic acid (BA) and ursolic acid (UA) [65]. UA can stop the cell cycle, induce apoptosis, scavenge free radicals and control several anti- and pro-apoptotic proteins. Furthermore, it is abundant in various fruits and vegetables. Additionally, in some human BC cells, UA has been demonstrated to have potent anti-inflammatory, anticancer, and antioxidant properties [8,64]. Palmitate is another component found in the HCT H fraction and has been associated with MDA-MB-231 cell apoptosis and phosphatidylinositol 3-kinase (PI3K) inhibition [66]. The components mentioned above might contribute to the anti-cancer properties in the H fraction.

The IC_{50} of HCT H fraction reflected a 50% inhibitory concentration of cell viability by MTT assay. IC_{50} induced cell apoptosis, whereas IC_{20} was less toxic. We have varied the concentrations from 0 to 400 μg/mL and found the cytotoxic effects in a dose-response manner. We selected IC_{20} (189 μg/mL) and IC_{50} (289 μg/mL) for further investigation of the molecular mechanisms according to our previous research data [46]. The results of annexin V/PI staining in MDA-MB-231 treated cells demonstrated that the percentage of early apoptotic cells increased dose-dependently. Our findings showed that the percentage of cells with MTP loss also increased dose-dependently, indicating the mitochondrial apoptosis pathway.

Caspase-induced apoptosis is mediated by both initiator caspases, such as caspase-8 and -9 for the extrinsic and intrinsic apoptosis pathways [67,68]. Activation of caspases-3, -6 and -7 resulting in apoptosis-related cellular morphological and biochemical characteristics [69]. The results exhibited that caspase-3 and -9 activities were activated in a concentration-dependent manner, especially at IC_{50}. The active caspase-8 cleaves Bid resulting in truncated Bid (tBid) and decreased level of Bid indicating apoptosis via both the death receptor and mitochondrial pathways [70–72]. Therefore, it indicated that H fraction-treated MDA-MB-231 cells underwent apoptosis via intrinsic and extrinsic pathways. However, we also used z-VAD-fmk (a pan-caspase inhibitor) pretreatment to suppress caspase activities to confirm apoptosis-regulated cell death via caspase activation [73]. The oligomerization of the Bax and Bak proteins on the outer mitochondrial membrane (OMM) is essential and allows the permeabilization of OMM [74]. The enhanced expression of both Bax and Bak cooperated with the increased percentage of cells with MTP loss. Besides, the down-regulation of anti-apoptotic Bcl-xL protein in the intrinsic pathway-mediated apoptosis was demonstrated.

Among cyclins/CDKs complexes, it was established that the D-type cyclins are expressed first, and form complexes with CDK4/CDK6 in the G1 checkpoint. We selected the cyclin D1/CDK4 complex as a representative in the G1 phase regulatory proteins because MDA-MB-231 cells induced by H fraction were arrested at G1. The cell population in the G1 phase was enhanced [75]. Downregulation of CDK4 and cyclin D1 expressions indicating the cell cycle arrest at the G1 phase corresponded to the cell cycle population histograms. Nonetheless, the p21 protein expression disappeared. The mutation of *p53* might accompany this. The absence of p21 expression might be caused by other signaling pathways activation, such as the MAPK/EGFR axis [72].

The cancer environment, including hypoxia and low nutrients, disrupts the endoplasmic reticulum's (ER) function, accumulating unfolded proteins and leading to UPR and ER stress [76,77]. Glucose-regulated protein 78 (GRP78) is the main chaperone protein with anti-apoptotic property, which involves newly synthesized polypeptide translocation across the ER membrane [78]. In addition to being a predictor of excellent prognosis in BC patients and a potential marker for chemotherapy response, GRP78 is a master regulator of ER stress that allows it to regulate the UPR signaling [79,80]. However, CHOP, one of the most well-characterized markers of ER stress, is established for its pro-apoptotic activity during ER stress [80]. Our findings showed that GRP78 and CHOP expression levels were upregulated in MDA-MB-231 treated cells. As a result, the H fraction sensitized MDA-MB-231 cells to ER stress-mediated apoptosis.

Hyperactivation of some signaling pathways promotes excess cell proliferation and exaggerates anti-apoptotic activity. The phosphoinositide 3-kinases (PI3Ks) are in a family of lipid kinases, whereas Akt (protein kinase B) is the key downstream effector of PI3K [81]. Akt signaling leads to cell cycle progression by phosphorylation which prevents cyclin D1 degradation and increases the translation of cyclin D1, D3, and E [82–84]. Furthermore, downregulation of the pAkt/Akt ratio causes inhibition of cell invasion, migration, metastasis and causes the dormant cell cycle [85]. Another signaling pathway, the ERK/MAPK axis is related to a wide variety of tumors such as ovarian, colon, breast and lung cancers [44,86]. Continual ERK/MAPK signaling activation promotes normal cells to become tumorous cells, while ERK/MAPK pathway inhibition restores tumor cells to a non-transformed state *in vitro* and *in vivo* [87]. Inhibition of ERK1/2 activity prevents colon cancer cells from entering the G1 phase into the S phase [87]. Besides, the relationship between PI3K signaling and the ERK pathway are associated with chemotherapy resistance [88]. pAkt/Akt ratio in H fraction-treated-MDA-MB-231 cells was reduced. These results corresponded to the decreased expression level of cyclin D1 and CDK4. Moreover, the pERK/ERK expression ratio decreased at IC_{20}, which enabled the cell cycle arrest at G1. Cell cycle arrest in the G1 phase is also caused by the downregulation of cyclin D1 and CDK4 protein expression [89]. The suppression of the ERK/MAPK signaling pathway enhances apoptosis induction by reducing downstream cell cycle regulatory protein in G1/S specific cyclin D1 and CDK4, corroborating the current findings [90]. The signaling pathway that regulates cell survival and proliferation is ERK/Akt/MAPK. Ras functions as an upstream activating molecule in this pathway, Raf acts as MAP3K, MAPK/ERK kinase (MEK), acts as MAPKK, and ERK

is the MAPK, establishing the Ras-Raf-MEK-ERK pathway because ERK is a member of the MAPK cascade [91]. Serine/threonine protein kinases of the ERK family are a sort of transducing pathway that delivers mitogen signals into cells, causing cells to divide [92]. This signaling cascade's attenuation causes BC cells to undergo controlled apoptosis. Even if the indicated pathways are established by the ERK/MAPK molecules, the p38 and JNK in the MAPK signaling can be distinguished and increased, whereas the ERK pathway is blocked, as in the C-phycocyanin-induced MDA-MB-231 cell apoptosis model [93].

This is the first study to look at the influence of the HCT H fraction on apoptosis induction in human BC MDA-MB-231 cells. The limitation of our study is time-consuming and uncertain about phytochemicals isolated from HCT. This problem can be solved by a molecular docking technique, which gives likely binding affinities between the receptors and phytochemicals. The stability of these phytochemicals is also another important factor. However, a comparison of HCT essential oils from various processing techniques (such as medicinal components and drying processes) and harvest seasons revealed a direct correlation between the chemical composition and quality of HCT and the pharmacological effects [94]. Developing stabilizers or coating by nanoparticles can promote compounds' stability and antioxidant potential. Moreover, these phytochemicals' bioavailability, pharmacokinetics and therapeutic efficacy remain unknown. In the therapeutic management of BC, their analogs may also play regulatory functions. For further research, it is required to compare each active compound's inhibitory impact and induction of apoptosis to a mixed mixture of the H fraction in cell lines and *in vivo* models (both animals and human-beings).

5. Conclusion

The results exhibited that HCT H fraction induced intrinsic pathway-mediated apoptosis in MDA-MB-231 cells by disrupting mitochondrial transmembrane potential (MTP) and increasing caspase-9 activation. The expression levels of pro-apoptotic proteins, viz., Bax and Bak were enhanced, whereas the anti-apoptotic protein Bcl-xL was decreased. The caspase-3 activity was elevated. The caspase-8 induction by an extrinsic pathway was cross-linked to the intrinsic pathway via Bid protein cleavage. The HCT H fraction also caused cell cycle arrest at the G1 phase by lowering cyclin D1 and CDK4 expression. Moreover, GRP78 and CHOP protein levels were upregulated, indicating an ER stress-mediated regulated cell death mechanism. The pro-survival Akt and ERK signaling pathways were blocked. As a result, the HCT H fraction triggered MDA-MB-231 apoptotic-regulated cell death via extrinsic, intrinsic and ER stress pathways and attenuated survival ERK/Akt signaling. The graphical abstract (Fig. 10) depicts the hypothesized visual pathway for HCT H fraction-induced MDA-MB-231 regulated cell death. This HCT H fraction therefore should receive more attention as a source for the future development of non-toxic chemopreventive agents against breast cancer.

Author contribution statement

Pitsinee Inthi: Conceived and designed the experiments; Performed the experiments; Analyzed and interpreted the data; Wrote the paper.

Hataichanok Pandith, Ph.D.: Analyzed and interpreted the data; Contributed reagents, materials, analysis tools or data.

Prachya Kongtawelert, Ph.D.: Contributed reagents, materials, analysis tools or data.

Subhawat Subhawa, Ph.D.: Performed the experiments; Analyzed and interpreted the data; Wrote the paper.

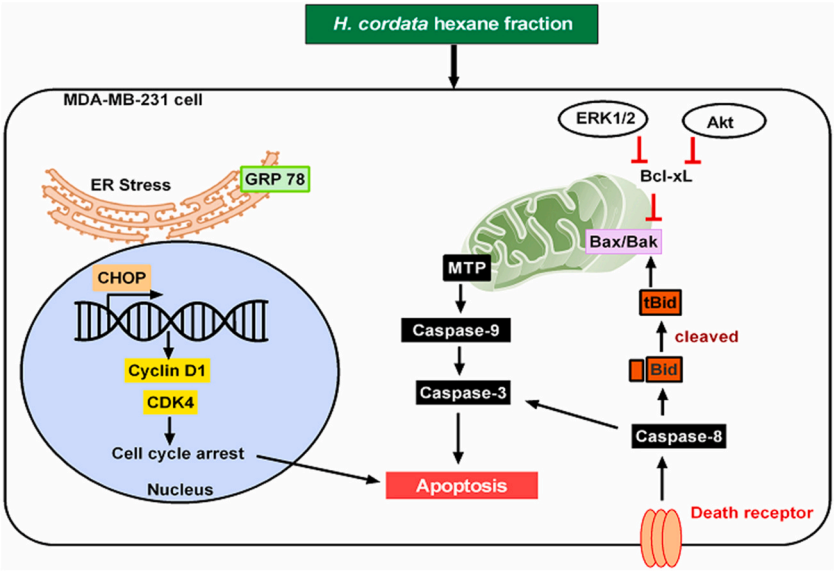

Fig. 10. The graphical abstract illustrates the mechanisms of *H. cordata* H fraction-induced MDA-MB-231 breast cancer cell apoptosis via extrinsic, intrinsic, ER stress pathways and attenuated ERK/Akt signaling axis.

Ratana Banjerdpongchai, MD, Ph.D.: Conceived and designed the experiments; Analyzed and interpreted the data; Contributed reagents, materials, analysis tools or data; Wrote the paper.

Data availability statement

Data will be made available on request.

Ethics approval

The study was cleared by Institutional Research Ethical Committee, (No. EXEMPTION: REC-25610515-13791, approved on 5 June 2018); Faculty of Medicine, Chiang Mai University, Chiang Mai, Thailand.

Consent to participate

Not applicable.

Funding

The study was supported by the Faculty of Medicine Research Fund, Research ID: BIO-2561-05490, Faculty of Medicine, Chiang Mai University, Chiang Mai, Thailand, grant number 16/2562.

Declaration of competing interest

The authors declare that they have no known competing financial interests or personal relationships that could have appeared to influence the work reported in this paper.

Appendix A. Supplementary data

Supplementary data to this article can be found online at https://doi.org/10.1016/j.heliyon.2023.e18755.

Abbreviations

AE, Ethyl acetate; Akt, Protein kinase B; ALA, α-linolenic acid; Bak, Bcl-2 homologous antagonist killer; Bax, Bcl-2-Associated X protein; BC, Breast cancer; Bcl-xL, B-cell lymphoma-extra large; Bid, BH3 interacting-domain death agonist; CHOP, Transcription factor C/EBP homologous protein; DDIT3, DNA damage-inducible transcript 3; Diablo, Direct inhibitor of apoptosis-binding protein (IAP) with low pI protein; ERK, Extracellular signal-regulated kinases; FADD, Fas-associated protein with death domain; FITC, Fluorescein isothiocyanate; Gadd153, Growth arrest and DNA damage gene 153; GC-MS, Gas chromatography-mass spectrometry; GRP78, Glucose-regulated protein 78; HCT, *Houttuynia cordata* Thunb.; JNK, Jun N-terminal kinase; MAPK, mitogen-activated protein kinases; MOMP, Mitochondrial outer membrane permeability; MTP, Mitochondrial transmembrane potential; MTT, 3-(4,5-Dimethylthiazol-2-yl)-2,5-diphenyltetrazolium bromide; pAkt, Phospho-Akt; pERK, Phospho-ERK; PI, Propidium iodide; RCD, Regulated cell death; SDS-PAGE, Sodium dodecyl sulphate–polyacrylamide gel electrophoresis; Smac, Second mitochondrial-derived activators of caspases; tBid, Truncated Bid; TNBC, Triple negative breast cancer; TTM, Thai traditional medicine.

References

[1] H. Sung, J. Ferlay, R.L. Siegel, M. Laversanne, I. Soerjomataram, A. Jemal, F. Bray, Global cancer statistics 2020: GLOBOCAN estimates of incidence and mortality worldwide for 36 cancers in 185 countries, CA A Cancer J. Clin. 71 (2021) 209–249.
[2] G.R. Brown, Breast cancer in transgender veterans: a ten-case series, LGBT Health 2 (2015) 77–80.
[3] A. Grundy, S.A. Harris, P.A. Demers, K.C. Johnson, D.A. Agnew, P.J. Villeneuve, Occupational exposure to magnetic fields and breast cancer among Canadian men, Cancer Med. 5 (2016) 586–596.
[4] P. Eroles, A. Bosch, J.A. Perez-Fidalgo, A. Lluch, Molecular biology in breast cancer: intrinsic subtypes and signaling pathways, Cancer Treat Rev. 38 (2012) 698–707.
[5] M. Fedele, L. Cerchia, G. Chiappetta, The epithelial-to-mesenchymal transition in breast cancer: focus on basal-like carcinomas, Cancers 9 (2017).
[6] J.S. Reis-Filho, L. Pusztai, Gene expression profiling in breast cancer: classification, prognostication, and prediction, Lancet (London, England) 378 (2011) 1812–1823.
[7] K.J. Chavez, S.V. Garimella, S. Lipkowitz, Triple negative breast cancer cell lines: one tool in the search for better treatment of triple negative breast cancer, Breast Dis. 32 (2010) 35–48.
[8] J. Iqbal, B.A. Abbasi, R. Batool, T. Mahmood, B. Ali, A.T. Khalil, S. Kanwal, S.A. Shah, R. Ahmad, Potential phytocompounds for developing breast cancer therapeutics: nature's healing touch, Eur. J. Pharmacol. 827 (2018) 125–148.
[9] N. Lumlerdkij, J. Tantiwongse, S. Booranasubkajorn, R. Boonrak, P. Akarasereenont, T. Laohapand, M. Heinrich, Understanding cancer and its treatment in Thai traditional medicine: an ethnopharmacological-anthropological investigation, J. Ethnopharmacol. 216 (2018) 259–273.
[10] B. Poonthananiwatkul, R.H. Lim, R.L. Howard, P. Pibanpaknitee, E.M. Williamson, Traditional medicine use by cancer patients in Thailand, J. Ethnopharmacol. 168 (2015) 100–107.

[11] J. Fu, L. Dai, Z. Lin, H. Lu, *Houttuynia cordata* Thunb: a review of phytochemistry and pharmacology and quality control, Chin. Med. 4 (2013) 101–123.
[12] T. Senawong, S. Saenglee, S. Misuna, J. Komaikul, G. Senawong, P. Wongphakham, S. Yunchalar, Phenolic acid composition and anticancer activity against human cancer cell lines of the commercially available fermentation products of *Houttuynia cordata*, Sci. Asia 40 (2014) 420–427.
[13] L. Yang, J.-G. Jiang, Bioactive components and functional properties of *Hottuynia cordata* and its applications, Pharmaceut. Biol. 47 (2009) 1154–1161.
[14] S. Rafiq, H. Hao, M. Ijaz, A. Raza, Pharmacological effects of *Houttuynia cordata* Thunb (*H. cordata*): a comprehensive review, Pharmaceuticals 15 (2022) 1079.
[15] R. Banjerdpongchai, P. Kongtawelert, Ethanolic extract of fermented Thunb induces human leukemic HL-60 and Molt-4 cell apoptosis via oxidative stress and a mitochondrial pathway, Asian Pac. J. Cancer Prev. APJCP : Asian Pac. J. Cancer Prev. APJCP 12 (2011) 2871–2874.
[16] P. Kumnerdkhonkaen, S. Saenglee, M.A. Asgar, G. Senawong, K. Khongsukwiwat, T. Senawong, Antiproliferative activities and phenolic acid content of water and ethanolic extracts of the powdered formula of *Houttuynia cordata* Thunb. fermented broth and Phyllanthus emblica Linn. fruit, BMC Compl. Alternative Med. 18 (2018) 1–12.
[17] Y.F. Chen, J.S. Yang, W.S. Chang, S.C. Tsai, S.F. Peng, Y.R. Zhou, *Houttuynia cordata* Thunb extract modulates G0/G1 arrest and Fas/CD95-mediated death receptor apoptotic cell death in human lung cancer A549 cells, J. Biomed. Sci. 20 (2013) 1–8.
[18] A. Prommaban, K. Kodchakorn, P. Kongtawelert, R. Banjerdpongchai, *Houttuynia cordata* Thunb fraction induces human leukemic Molt-4 cell apoptosis through the endoplasmic reticulum stress pathway, Asian Pac. J. Cancer Prev. APJCP : Asian Pac. J. Cancer Prev. APJCP 13 (2012) 1977–1981.
[19] S. Subhawa, T. Chewonarin, R. Banjerdpongchai, The effects of Houttuynia cordata Thunb and piper ribesioides wall extracts on breast carcinoma cell proliferation, migration, invasion and apoptosis, Molecules 25 (2020).
[20] J.M. Chun, K.J. Nho, H.S. Kim, A.Y. Lee, B.C. Moon, H.K. Kim, An ethyl acetate fraction derived from *Houttuynia cordata* extract inhibits the production of inflammatory markers by suppressing NF-κB and MAPK activation in lipopolysaccharide-stimulated RAW 264.7 macrophages, BMC Compl. Alternative Med. 14 (2014) 1–11.
[21] A.L. Waterhouse, Determination of total phenolics, Current Protocols in Food Analytical Chemistry 6 (2002) 1–8.
[22] R. Banjerdpongchai, P. Kongtawelert, O. Khantamat, C. Srisomsap, D. Chokchaichamnankit, P. Subhasitanont, J. Svasti, Mitochondrial and endoplasmic reticulum stress pathways cooperate in zearalenone-induced apoptosis of human leukemic cells, J. Hematol. Oncol. 3 (2010) 50.
[23] R. Banjerdpongchai, B. Wudtiwai, P. Khaw-On, W. Rachakhom, N. Duangnil, P. Kongtawelert, Hesperidin from Citrus seed induces human hepatocellular carcinoma HepG2 cell apoptosis via both mitochondrial and death receptor pathways, Tumour Biol 37 (2016) 227–237.
[24] R. Banjerdpongchai, P. Khaw-On, C. Ristee, W. Pompimon, 6,8-dihydroxy-7-methoxy-1-methyl-azafluorenone induces caspase-8- and -9-mediated apoptosis in human cancer cells, Asian Pac. J. Cancer Prev. APJCP : Asian Pac. J. Cancer Prev. APJCP 14 (2013) 2637–2641.
[25] R. Banjerdpongchai, Y. Chanwikruy, V. Rattanapanone, B. Sripanidkulchai, Induction of apoptosis in the human Leukemic U937 cell line by Kaempferia parviflora Wall.ex.Baker extract and effects of paclitaxel and camptothecin, Asian Pac. J. Cancer Prev. APJCP : Asian Pac. J. Cancer Prev. APJCP 10 (2009) 1137–1140.
[26] R. Yapasert, N. Lertprasertsuk, S. Subhawa, J. Poofery, B. Sripanidkulchai, R. Banjerdpongchai, Antitumor efficacy of the herbal recipe benja amarit against highly invasive cholangiocarcinoma by inducing apoptosis both in vitro and in vivo, Int. J. Mol. Sci. 21 (2020).
[27] J. Poofery, B. Sripanidkulchai, R. Banjerdpongchai, Extracts of Bridelia ovata and Croton oblongifolius induce apoptosis in human MDA-MB-231 breast cancer cells via oxidative stress and mitochondrial pathways, Int. J. Oncol. 56 (2020) 969–985.
[28] C.M. Pfeffer, A.T.K. Singh, Apoptosis: a target for anticancer therapy, Int. J. Mol. Sci. 19 (2018) 1–10.
[29] L. Galluzzi, I. Vitale, S.A. Aaronson, J.M. Abrams, D. Adam, P. Agostinis, E.S. Alnemri, L. Altucci, I. Amelio, D.W. Andrews, M. Annicchiarico-Petruzzelli, A. V. Antonov, E. Arama, E.H. Baehrecke, N.A. Barlev, N.G. Bazan, F. Bernassola, M.J.M. Bertrand, K. Bianchi, M.V. Blagosklonny, K. Blomgren, C. Borner, P. Boya, C. Brenner, M. Campanella, E. Candi, D. Carmona-Gutierrez, F. Cecconi, F.K. Chan, N.S. Chandel, E.H. Cheng, J.E. Chipuk, J.A. Cidlowski, A. Ciechanover, G. M. Cohen, M. Conrad, J.R. Cubillos-Ruiz, P.E. Czabotar, V. D'Angiolella, T.M. Dawson, V.L. Dawson, V. De Laurenzi, R. De Maria, K.M. Debatin, R. J. DeBerardinis, M. Deshmukh, N. Di Daniele, F. Di Virgilio, V.M. Dixit, S.J. Dixon, C.S. Duckett, B.D. Dynlacht, W.S. El-Deiry, J.W. Elrod, G.M. Fimia, S. Fulda, A.J. Garcia-Saez, A.D. Garg, C. Garrido, E. Gavathiotis, P. Golstein, E. Gottlieb, D.R. Green, L.A. Greene, H. Gronemeyer, A. Gross, G. Hajnoczky, J.M. Hardwick, I.S. Harris, M.O. Hengartner, C. Hetz, H. Ichijo, M. Jaattela, B. Joseph, P.J. Jost, P.P. Juin, W.J. Kaiser, M. Karin, T. Kaufmann, O. Kepp, A. Kimchi, R.N. Kitsis, D. J. Klionsky, R.A. Knight, S. Kumar, S.W. Lee, J.J. Lemasters, B. Levine, A. Linkermann, S.A. Lipton, R.A. Lockshin, C. Lopez-Otin, S.W. Lowe, T. Luedde, E. Lugli, M. MacFarlane, F. Madeo, M. Malewicz, W. Malorni, G. Manic, J.C. Marine, S.J. Martin, J.C. Martinou, J.P. Medema, P. Mehlen, P. Meier, S. Melino, E.A. Miao, J.D. Molkentin, U.M. Moll, C. Munoz-Pinedo, S. Nagata, G. Nunez, A. Oberst, M. Oren, M. Overholtzer, M. Pagano, T. Panaretakis, M. Pasparakis, J. M. Penninger, D.M. Pereira, S. Pervaiz, M.E. Peter, M. Piacentini, P. Pinton, J.H.M. Prehn, H. Puthalakath, G.A. Rabinovich, M. Rehm, R. Rizzuto, C.M. P. Rodrigues, D.C. Rubinsztein, T. Rudel, K.M. Ryan, E. Sayan, L. Scorrano, F. Shao, Y. Shi, J. Silke, H.U. Simon, A. Sistigu, B.R. Stockwell, A. Strasser, G. Szabadkai, S.W.G. Tait, D. Tang, N. Tavernarakis, A. Thorburn, Y. Tsujimoto, B. Turk, T. Vanden Berghe, P. Vandenabeele, M.G. Vander Heiden, A. Villunger, H.W. Virgin, K.H. Vousden, D. Vucic, E.F. Wagner, H. Walczak, D. Wallach, Y. Wang, J.A. Wells, W. Wood, J. Yuan, Z. Zakeri, B. Zhivotovsky, L. Zitvogel, G. Melino, G. Kroemer, Molecular mechanisms of cell death: recommendations of the nomenclature committee on cell death, Cell Death Differ. 25 (2018) 486–541.
[30] J. Suzuki, E. Imanishi, S. Nagata, Exposure of phosphatidylserine by Xk-related protein family members during apoptosis, J. Biol. Chem. 289 (2014) 30257–30267.
[31] L. Galluzzi, O. Kepp, G. Kroemer, Mitochondrial regulation of cell death: a phylogenetically conserved control, Microbial cell (Graz, Austria) 3 (2016) 101–108.
[32] R.S.Y. Wong, Apoptosis in cancer: from pathogenesis to treatment, J. Exp. Clin. Cancer Res. 30 (2011) 1–14.
[33] X. Xu, Y. Lai, Z.C. Hua, Apoptosis and apoptotic body: disease message and therapeutic target potentials, Biosci. Rep. 39 (2019) 1–17.
[34] S. McComb, P.K. Chan, A. Guinot, H. Hartmannsdottir, S. Jenni, M.P. Dobay, J.-P. Bourquin, B.C. Bornhauser, Efficient apoptosis requires feedback amplification of upstream apoptotic signals by effector caspase-3 or -7, Sci. Adv. 5 (2019), eaau9433.
[35] D.R. McIlwain, T. Berger, T.W. Mak, Caspase functions in cell death and disease, Cold Spring Harbor Perspect. Biol. 5 (2013), a008656.
[36] H. Kalkavan, D.R. Green, MOMP, cell suicide as a BCL-2 family business, Cell Death Differ. 25 (2018) 46–55.
[37] C.J. Sherr, Surprising regulation of cell cycle entry, Science 366 (2019) 1315–1316.
[38] H. Skomedal, G.B. Kristensen, A.K. Lie, R. Holm, Aberrant expression of the cell cycle associated proteins TP53, MDM2, p21, p27, cdk4, cyclin D1, RB, and EGFR in cervical carcinomas, Gynecol. Oncol. 73 (1999) 223–228.
[39] P. Dauer, N.S. Sharma, V.K. Gupta, B. Durden, R. Hadad, S. Banerjee, V. Dudeja, A. Saluja, S. Banerjee, ER stress sensor, glucose regulatory protein 78 (GRP78) regulates redox status in pancreatic cancer thereby maintaining "stemness", Cell Death Dis. 10 (2019) 1–13.
[40] R. Jäger, M.J. Bertrand, A.M. Gorman, P. Vandenabeele, A. Samali, The unfolded protein response at the crossroads of cellular life and death during endoplasmic reticulum stress, Biol. Cell. 104 (2012) 259–270.
[41] D. Hanahan, L.M. Coussens, Accessories to the crime: functions of cells recruited to the tumor microenvironment, Cancer Cell 21 (2012) 309–322.
[42] D. Hanahan, R.A. Weinberg, Hallmarks of cancer: the next generation, Cell 144 (2011) 646–674.
[43] Y. Fong, C.-Y. Wu, K.-F. Chang, B.-H. Chen, W.-J. Chou, C.-H. Tseng, Y.-C. Chen, H.-M.D. Wang, Y.-L. Chen, C.-C. Chiu, Dual roles of extracellular signal-regulated kinase (ERK) in quinoline compound BPIQ-induced apoptosis and anti-migration of human non-small cell lung cancer cells, Cancer Cell Int. 17 (2017) 37.
[44] Y.-J. Guo, W.-W. Pan, S.-B. Liu, Z.-F. Shen, Y. Xu, L.-L. Hu, ERK/MAPK signalling pathway and tumorigenesis, Exp. Ther. Med. 19 (2020) 1997–2007.
[45] E. Paplomata, R. O'Regan, The PI3K/AKT/mTOR pathway in breast cancer: targets, trials and biomarkers, Ther Adv Med Oncol 6 (2014) 154–166.
[46] B. Wudtiwai, P. Pitchakarn, R. Banjerdpongchai, Alpha-mangostin, an active compound in Garcinia mangostana, abrogates anoikis-resistance in human hepatocellular carcinoma cells, Toxicol. Vitro : an international journal published in association with BIBRA 53 (2018) 222–232.
[47] N.-N. Zhou, J. Tang, W.-D. Chen, G.-K. Feng, B.-F. Xie, Z.-C. Liu, D. Yang, X.-F. Zhu, Houttuyninum, an active constituent of Chinese herbal medicine, inhibits phosphorylation of HER2/neu receptor tyrosine kinase and the tumor growth of HER2/neu-overexpressing cancer cells, Life Sci. 90 (2012) 770–775.
[48] L. Gao, R.-Y. Gui, X.-N. Zheng, Y.-X. Wang, Y. Gong, T. Wang, J. Wang, J. Huang, X.-H. Liao, Topical Application of *Houttuynia cordata* Thunb Ethanol Extracts Increases Tumor Infiltrating CD8+/Treg Cells Ratio and Inhibits Cutaneous Squamous Cell Carcinoma *in Vivo*, 2021.

[49] S. Subhawa, A. Naiki-Ito, H. Kato, T. Naiki, M. Komura, A. Nagano-Matsuo, R. Yeewa, S. Inaguma, T. Chewonarin, R. Banjerdpongchai, S. Takahashi, Suppressive effect and molecular mechanism of *Houttuynia cordata* Thunb. Extract against prostate carcinogenesis and castration-resistant prostate cancer, Cancers 13 (2021).
[50] J.M. Kim, I.H. Hwang, I.S. Jang, M. Kim, I.S. Bang, S.J. Park, Y.J. Chung, J.C. Joo, M.G. Lee, *Houttuynia cordata* Thunb promotes activation of HIF-1A-FOXO3 and MEF2A pathways to induce apoptosis in human HepG2 hepatocellular carcinoma cells, Integr. Cancer Ther. 16 (2017) 360–372.
[51] T.Q. Nguyen, H.N.M. Nguyen, V.M. Le, D.-H. Ngo, T.S. Vo, Inhibition of cell proliferation by *Houttuynia cordata* extract on gastric cancer cells via induction of apoptosis, Journal of Pharmaceutical Research International 34 (2022) 65–72.
[52] G.H. Lai, F. Wang, D.R. Nie, S.J. Lei, Z.J. Wu, J.X. Cao, Identifying active substances and the pharmacological mechanism of *Houttuynia cordata* Thunb. In treating radiation-induced lung injury based on network pharmacology and molecular docking verification, evidence-based complementary and alternative medicine, eCAM 2022 (2022), 3776340.
[53] S.K. Das, S.J. Deka, D. Paul, D.D. Gupta, T.J. Das, D.K. Maravi, H. Tag, P.K. Hui, In-silico based identification of phytochemicals from *Houttuynia cordata* Thunb. as potential inhibitors for overexpressed HER2 and VEGFR2 cancer genes, J. Biomol. Struct. Dyn. 40 (2022) 6857–6867.
[54] L. He, Sodium new houttuyfonate induces apoptosis of breast cancer cells via ROS/PDK1/AKT/GSK3β Axis, Cancers 15 (2023) 1614.
[55] C. Laldinsangi, The therapeutic potential of *Houttuynia cordata*: a current review, Heliyon 8 (2022), e10386.
[56] C.J. Fabian, B.F. Kimler, S.D. Hursting, Omega-3 fatty acids for breast cancer prevention and survivorship, Breast cancer research, BCR 17 (2015) 1–11.
[57] J.K. Mason, S. Klaire, S. Kharotia, A.K. Wiggins, L.U. Thompson, α-linolenic acid and docosahexaenoic acid, alone and combined with trastuzumab, reduce HER2-overexpressing breast cancer cell growth but differentially regulate HER2 signaling pathways, Lipids Health Dis. 14 (2015) 1–10.
[58] A.K. Wiggins, S. Kharotia, J.K. Mason, L.U. Thompson, α-Linolenic acid reduces growth of both triple negative and luminal breast cancer cells in high and low estrogen environments, Nutr. Cancer 67 (2015) 1001–1009.
[59] R. Deshpande, P. Mansara, S. Suryavanshi, R. Kaul-Ghanekar, Alpha-linolenic acid regulates the growth of breast and cervical cancer cell lines through regulation of NO release and induction of lipid peroxidation, J. Mol. Biochem. 2 (2013) 6–17.
[60] M. Majeed, R. Rehman, Manipulation of Key Genes Involved in Biosynthesis of Terpenoid Compounds in Plants, 2022, pp. 285–300.
[61] S.B. Ateba, M.A. Mvondo, S.T. Ngeu, J. Tchoumtchoua, C.F. Awounfack, D. Njamen, L. Krenn, Natural terpenoids against female breast cancer: a 5-year recent research, Curr. Med. Chem. 25 (2018) 3162–3213.
[62] J. Cai, Y.Y. Zhong, S. Tian, Naturally occurring davanone terpenoid exhibits anticancer potential against ovarian cancer cells by inducing programmed cell death, by inducing caspase-dependent apoptosis, loss of mitochondrial membrane potential, inhibition of cell migration and invasion and targeting PI3K/AKT/MAPK signaling pathway, Journal of BUON 25 (2020) 2301–2307.
[63] B. Chakravarti, R. Maurya, J.A. Siddiqui, H.K. Bid, S.M. Rajendran, P.P. Yadav, R. Konwar, In vitro anti-breast cancer activity of ethanolic extract of Wrightia tomentosa: role of pro-apoptotic effects of oleanolic acid and urosolic acid, J. Ethnopharmacol. 142 (2012) 72–79.
[64] J. Iqbal, B.A. Abbasi, R. Ahmad, T. Mahmood, S. Kanwal, B. Ali, A.T. Khalil, S.A. Shah, M.M. Alam, H. Badshah, Ursolic acid a promising candidate in the therapeutics of breast cancer: current status and future implications, Biomedicine & pharmacotherapy = Biomedecine & pharmacotherapie 108 (2018) 752–756.
[65] V. Mishra, A. Soren, A. Yadav, Toxicological Evaluations of Betulinic Acid and Ursolic Acid; Common Constituents of *Houttuynia cordata* Used as an Anthelmintic by the Naga Tribes in North-east India, 2021.
[66] S. Hardy, Y. Langelier, M. Prentki, Oleate activates phosphatidylinositol 3-kinase and promotes proliferation and reduces apoptosis of MDA-MB-231 breast cancer cells, whereas palmitate has opposite effects, Cancer Res. 60 (2000) 6353–6358.
[67] Y. Zhao, X. Sui, H. Ren, From procaspase-8 to caspase-8: revisiting structural functions of caspase-8, J. Cell. Physiol. 225 (2010) 316–320.
[68] M.L. Würstle, M.A. Laussmann, M. Rehm, The central role of initiator caspase-9 in apoptosis signal transduction and the regulation of its activation and activity on the apoptosome, Exp. Cell Res. 318 (2012) 1213–1220.
[69] M.Y. Seo, K. Rhee, Caspase-mediated cleavage of the centrosomal proteins during apoptosis, Cell Death Dis. 9 (2018) 571–582.
[70] C. Kantari, H. Walczak, Caspase-8 and Bid: caught in the act between death receptors and mitochondria, Biochim. Biophys. Acta Mol. Cell Res. 1813 (2011) 558–563.
[71] P. Khaw-on, R. Banjerdpongchai, Induction of intrinsic and extrinsic apoptosis pathways in the human leukemic MOLT-4 cell line by terpinen-4-ol, Asian Pac. J. Cancer Prev. APJCP : Asian Pac. J. Cancer Prev. APJCP 13 (2012) 3073–3076.
[72] W. Rachakhom, P. Khaw-On, W. Pompimon, R. Banjerdpongchai, Dihydrochalcone derivative induces breast cancer cell apoptosis via intrinsic, extrinsic, and ER stress pathways but abolishes EGFR/MAPK pathway, BioMed Res. Int. 2019 (2019), 7298539.
[73] D. Chauvier, S. Ankri, C. Charriaut-Marlangue, R. Casimir, E. Jacotot, Broad-spectrum caspase inhibitors: from myth to reality? Cell Death Differ. 14 (2007) 387–391.
[74] D. Westphal, G. Dewson, P.E. Czabotar, R.M. Kluck, Molecular biology of Bax and Bak activation and action, Biochim. Biophys. Acta 1813 (2011) 521–531.
[75] A. Uzman, Molecular biology of the cell, in: Biochemistry and Molecular Biology Education, fourth ed. 31, 2003, pp. 212–214.
[76] R. Sano, J.C. Reed, ER stress-induced cell death mechanisms, Biochim. Biophys. Acta 1833 (2013) 3460–3470.
[77] A. Schonthal, Endoplasmic reticulum stress: its role in disease and novel prospects for therapy, Sci. Tech. Rep. (2012), 857516.
[78] K.-W. Park, G. Eun Kim, R. Morales, F. Moda, I. Moreno-Gonzalez, L. Concha-Marambio, A.S. Lee, C. Hetz, C. Soto, The endoplasmic reticulum chaperone GRP78/BiP modulates prion propagation in vitro and in vivo, Sci. Rep. 7 (2017), 44723.
[79] K. Shi, D. Wang, X. Cao, Y. Ge, Endoplasmic reticulum stress signaling is involved in mitomycin C (MMC)-induced apoptosis in human fibroblasts via PERK pathway, PLoS One 8 (2013), e59330.
[80] R. Yapasert, B. Sripanidkulchai, M. Teerachaisakul, K. Banchuen, R. Banjerdpongchai, Anticancer effects of a traditional Thai herbal recipe Benja Amarit extracts against human hepatocellular carcinoma and colon cancer cell by targeting apoptosis pathways, J. Ethnopharmacol. 254 (2020), 112732.
[81] P. Xia, X.Y. Xu, PI3K/Akt/mTOR signaling pathway in cancer stem cells: from basic research to clinical application, American journal of cancer research 5 (2015) 1602–1609.
[82] R.C. Muise-Helmericks, H.L. Grimes, A. Bellacosa, S.E. Malstrom, P.N. Tsichlis, N. Rosen, Cyclin D expression is controlled post-transcriptionally via a phosphatidylinositol 3-kinase/Akt-dependent pathway, J. Biol. Chem. 273 (1998) 29864–29872.
[83] T. Shimura, Targeting the AKT/cyclin D1 pathway to overcome intrinsic and acquired radioresistance of tumors for effective radiotherapy, Int. J. Radiat. Biol. 93 (2017) 381–385.
[84] S.M. Nur Husna, H.T. Tan, R. Mohamud, A. Dyhl-Polk, K.K. Wong, Inhibitors targeting CDK4/6, PARP and PI3K in breast cancer: a review, Ther Adv Med Oncol 10 (2018) 1–21.
[85] S.R. Hosford, T.W. Miller, Clinical potential of novel therapeutic targets in breast cancer: CDK4/6, Src, JAK/STAT, PARP, HDAC, and PI3K/AKT/mTOR pathways, Pharmacogenomics Personalized Med. 7 (2014) 203–215.
[86] L. Li, G.D. Zhao, Z. Shi, L.L. Qi, L.Y. Zhou, Z.X. Fu, The Ras/Raf/MEK/ERK signaling pathway and its role in the occurrence and development of HCC, Oncol. Lett. 12 (2016) 3045–3050.
[87] J.S. Sebolt-Leopold, D.T. Dudley, R. Herrera, K. Van Becelaere, A. Wiland, R.C. Gowan, H. Tecle, S.D. Barrett, A. Bridges, S. Przybranowski, W.R. Leopold, A. R. Saltiel, Blockade of the MAP kinase pathway suppresses growth of colon tumors in vivo, Nat. Med. 5 (1999) 810–816.
[88] M. Martini, M.C. De Santis, L. Braccini, F. Gulluni, E. Hirsch, PI3K/AKT signaling pathway and cancer: an updated review, Ann. Med. 46 (2014) 372–383.
[89] S.L. Sammons, D.L. Topping, K.L. Blackwell, HR+, HER2- advanced breast cancer and CDK4/6 inhibitors: mode of action, clinical activity, and safety profiles, Curr. Cancer Drug Targets 17 (2017) 637–649.
[90] K. Maemura, N. Shiraishi, K. Sakagami, K. Kawakami, T. Inoue, M. Murano, M. Watanabe, Y. Otsuki, Proliferative effects of gamma-aminobutyric acid on the gastric cancer cell line are associated with extracellular signal-regulated kinase 1/2 activation, J. Gastroenterol. Hepatol. 24 (2009) 688–696.
[91] S. Yang, G. Liu, Targeting the Ras/Raf/MEK/ERK pathway in hepatocellular carcinoma, Oncol. Lett. 13 (2017) 1041–1047.

[92] R. Anjum, J. Blenis, The RSK family of kinases: emerging roles in cellular signalling, Nat. Rev. Mol. Cell Biol. 9 (2008) 747–758.
[93] L. Jiang, Y. Wang, G. Liu, H. Liu, F. Zhu, H. Ji, B. Li, C-Phycocyanin exerts anti-cancer effects via the MAPK signaling pathway in MDA-MB-231 cells, Cancer Cell Int. 18 (2018) 12.
[94] X. Pan, H. Li, D. Chen, J. Zheng, L. Yin, J. Zou, Y. Zhang, K. Deng, M. Xiao, L. Meng, F. He, Comparison of essential oils of *Houttuynia cordata* Thunb. From different processing methods and harvest seasons based on GC-MS and chemometric analysis, International journal of analytical chemistry 2021 (2021), 8324169.